AD-A042 969 AEROSPACE CORP EL SEGUNDO CALIF VEHICLE ENGINEERING DIV F/G 20/4
NUMERICAL INVESTIGATION OF NONLINEAR WAVE INTERACTION IN A TWO---ETC(U)
JUN 77 J W MURDOCK, T D TAYLOR F04701-76-C-0077
UNCLASSIFIED TR-0077(2729)-1 SAMSO-TR-77-115 NL

1 OF 1
ADA042 969

END
DATE FILMED
9-77
DDC

REPORT SAMSO-TR-77 -115



# Numerical Investigation of Nonlinear Wave Interaction in a Two-Dimensional Boundary Layer

Vehicle Engineering Division
Engineering Science Operations
The Aerospace Corporation
El Segundo, Calif. 90245

27 June 1977

Final Report



Sponsored by
DEFENSE ADVANCED RESEARCH PROJECTS AGENCY (DoD)
and
OFFICE OF NAVAL RESEARCH (ONR)

Monitored by SAMSO under Contract No. F04701-76-C-0077

This final report was submitted by The Aerospace Corporation, El Segundo, CA 90245, under Contract F04701-76-C-0077 with the Space and Missile Systems Organization, P.O. Box 92960, Worldway Postal Center, Los Angeles, CA 90009. It was reviewed and approved for The Aerospace Corporation by E.G. Hertler, Engineering Science Operations. Mr. R.D. Cooper, Office of Naval Research was the project engineer.

This report has been reviewed by the Information Office (OI) and is releasable to the National Technical Information Service (NTIS). At NTIS, it will be available to the general public, including foreign nations.

This technical report has been reviewed and is approved for publication.

GERHARD E. AICHINGER
Technical Advisor
Contracts Management Office

FOR THE COMMANDER

FRANK J. BANE
Chief, Contracts Management Office

UNCLASSIFIED

SECURITY CLASSIFICATION OF THIS PAGE *(When Data Entered)*

| REPORT DOCUMENTATION PAGE | READ INSTRUCTIONS BEFORE COMPLETING FORM |
|---|---|
| 1. REPORT NUMBER: SAMSO-TR-77-115 | 2. GOVT ACCESSION NO. / 3. RECIPIENT'S CATALOG NUMBER |
| 4. TITLE *(and Subtitle)*: Numerical Investigation of Nonlinear Wave Interaction in a Two-Dimensional Boundary Layer. | 5. TYPE OF REPORT & PERIOD COVERED: Final rept. |
| | 6. PERFORMING ORG. REPORT NUMBER: TR-0077(2729)-1 |
| 7. AUTHOR(s): John W. Murdock and Thomas D. Taylor | 8. CONTRACT OR GRANT NUMBER(s): F04701-76-C-0077 |
| 9. PERFORMING ORGANIZATION NAME AND ADDRESS: The Aerospace Corporation, El Segundo, Calif. 90245 | 10. PROGRAM ELEMENT, PROJECT, TASK AREA & WORK UNIT NUMBERS: 22 Jun 77 |
| 11. CONTROLLING OFFICE NAME AND ADDRESS: Defense Advanced Research Projects Agency, 1400 Wilson Blvd., Arlington, Va. 22209 | 12. REPORT DATE: 27 ~~May~~ JUNE 1977 |
| | 13. NUMBER OF PAGES: 31 |
| 14. MONITORING AGENCY NAME & ADDRESS *(if different from Controlling Office)*: Space and Missile Systems Organization, Air Force Systems Command, Los Angeles, Calif. 90009 | 15. SECURITY CLASS. *(of this report)*: Unclassified |
| | 15a. DECLASSIFICATION/DOWNGRADING SCHEDULE |

16. DISTRIBUTION STATEMENT *(of this Report)*

Approved for public release; distribution unlimited (12) 33p.

17. DISTRIBUTION STATEMENT *(of the abstract entered in Block 20, if different from Report)*

18. SUPPLEMENTARY NOTES

19. KEY WORDS *(Continue on reverse side if necessary and identify by block number)*

Boundary-Layer Transition
Unsteady Flow
Nonlinear Waves
Computational Methods

20. ABSTRACT *(Continue on reverse side if necessary and identify by block number)*

A spectral method is used to solve for the unsteady, two-dimensional flow over a flat plate in the Reynolds number range of transition. The physical problem considered is the propagation of large amplitude (nonlinear) Tollmien-Schlichting waves in a boundary layer. The solutions are generally in qualitative agreement with nonlinear stability theories in that: (1) nonlinear effects can be destabilizing, (2) the growth/decay behavior of the primary mode is changed only slightly by nonlinear effects, and → next page

DD FORM 1473 (FACSIMILE)

UNCLASSIFIED

409 369

SECURITY CLASSIFICATION OF THIS PAGE *(When Data Entered)*

19. KEY WORDS *(Continued)*

20. ABSTRACT *(Continued)*

(3) the second temporal harmonic is usually a second spatial harmonic. There are, however, regions in the flow in which both (1) and (3) are not true. Details of the solution in such a region are given to illustrate the complex nonlinear wave interactions possible in a boundary layer.

CONTENTS

## FIGURES

## 1. INTRODUCTION

An important engineering problem which occurs in many internal and external flow situations is laminar to turbulent transition. Although there appears to be a variety of physical mechanisms which may lead to boundary layer transition, only one is even partially understood in theoretical terms. This mechanism, the growth of linear Tollmien-Schlichting waves in a boundary layer, can lead to transition as shown, for example, by the data of Klebanoff, Tidstrom and Sargent[1]. The growth of small amplitude Tollmien-Schlichting waves in a boundary layer is reasonably well described by the usual Orr-Sommerfeld equation; the recent work of Bouthier[2], Gaster[3], and Saric and Nayfeh[4] improves the agreement by taking account of nonparallel effects in the boundary layer. The data of Klebanoff, Tidstrom and Sargent show that after the linear amplification of the Tollmien-Schlichting waves, three-dimensional and nonlinear effects become important, leading to a secondary instability and then transition.

This report describes the results of numerical calculations similar to the laboratory experiments of Klebanoff, Tidstrom and Sargent[1], except for the fact that the calculations are confined to two space dimensions. There are no other restrictions; the disturbance need not be small as no linearization is performed, and the full equations are solved so the flow is automatically nonparallel. The numerical computations are similar to laboratory experiments in that Tollmien-Schlichting waves of varying amplitudes are

---

[1] Klebanoff, P.S., K.D. Tidstrom and L.M. Sargent, "The Three-Dimensional Nature of Boundary Layer Instability," J. Fluid Mech., Vol. 12, 1962, pp. 1-34.

[2] Bouthier, Michel, "Stabilité Linéaire des Écoulements Presque Parallèles," J. de Mécanique, Vol. 11, No. 4, December 1972, pp. 599-621 and Vol. 12, No. 1, March 1973, pp. 75-95.

[3] Gaster, M., "On the Effects of Boundary-Layer Growth on the Flow-Stability," J. Fluid Mech., Vol. 66, 1974, pp. 465-480.

[4] Saric, W.S. and A.H. Nayfeh, Virginia Polytechnic Institute and State University, "Non-Parallel Stability of Boundary-Layer Flows," 1975, VPI-E-75-5.

propagated in a Blasius boundary layer. The fact that the calculation is two-dimensional has the disadvantage that it cannot predict the three-dimensional data. On the other hand, it is advantageous to be able to investigate the nonlinear interactions without the complications of a third dimension. It also allows qualitative comparisons with nonlinear stability theory (see Stewartson[5] for a recent review of this subject). The comparisons can only be qualitative because the nonlinear stability analyses known to these authors are only for parallel flows (such as Couette flow) and are valid only in the vicinity of the critical Reynolds number.

Studies of boundary-layer stability similar to the present work have been carried out by Fasel[6, 7]. His published work describes solutions to the unsteady Navier-Stokes equations in which the amplitude of the disturbance is small and, therefore, nonlinear effects are unimportant. However, he has indicated in a private communication that he has also obtained solutions in which nonlinear effects are present and found these solutions qualitatively similar to the results of Murdock[8].

This report describes a portion of an extended numerical study of Blasius boundary layer in the Reynolds number range of transition. An earlier paper by Murdock[8] gives a more detailed description of the formulation, the assumptions and the numerics as well as some of the early results. Additional numerical results are presented herein.

---

[5] Stewartson, K., "Some Aspects of Nonlinear Stability Theory," Polish Academy of Sciences, Vol. 7, 1975, pp. 101-128.

[6] Fasel, Hermann F., "Numerical Solution of the Unsteady Navier-Stokes Equations for the Investigation of Laminar Boundary Layer Stability," Proceedings of the Fourth International Conference on Numerical Methods in Fluid Dynamics, Springer-Verlag, Berlin, 1974, pp. 151-160.

[7] Fasel, Hermann F., "Investigation of the Stability of Boundary Layers by a Finite-Difference Model of the Navier-Stokes Equations," J. Fluid Mech., Vol. 78, 1976, pp. 355-383.

[8] Murdock, John W., "A Numerical Study of Nonlinear Effects on Boundary-Layer Stability," AIAA 15th Aerospace Sciences Meeting, Paper 77-127, Submitted to the AIAA Journal.

## 2. PROBLEM FORMULATION

The equations which are solved together with the boundary conditions are given in this section for completeness.

The equations are solved in dimensionless parabolic coordinates $\xi$ and $\eta$, which are related to the dimensional Cartesian coordinates, x and y, as follows

$$x + iy = x_1 \left[ \xi + i\eta \left( 2R_{x_1} \right)^{-1/2} \right]^2 \tag{1}$$

where $x_1$ is a typical distance from the leading edge, and $R_{x_1}$ is the Reynolds number based on freestream velocity and $x_1$. The time is made dimensionless with the freestream velocity and with $x_1$

$$\tau = tU_\infty / x_1 . \tag{2}$$

The stream function and vorticity are the dependent variables, and dimensionless versions of these variables are defined in terms of the dimensional quantities $\psi$ and $\omega$.

$$\psi = (2\nu U_\infty x_1)^{1/2} \xi f = (2\nu U_\infty x_1)^{1/2} g \tag{3}$$

$$\omega = U_\infty [U_\infty / (2\nu x_1)]^{1/2} \Omega / \xi \tag{4}$$

where $\nu$ is the kinematic viscosity. The dependent variable f reduces to the usual Blasius dimensionless stream function when the solution is not a function of $\xi$ and $\tau$.

The equations solved are a slightly simplified version of the Navier-Stokes equations referred to as the parabolized vorticity equations (see Ref. 8).

$$2\xi\Omega_{\tau} = \Omega_{\eta\eta}/\xi + g_{\xi}\Omega_{\eta}/\xi - g_{\eta}(\Omega/\xi)_{\xi} + \left[ g_{\eta\eta}\Big/\left(2\xi^{2}R_{x_1}\right)\right]_{\xi\xi} \tag{5}$$

$$\xi\,\Omega = g_{\eta\eta} + g_{\xi\xi}\Big/\left(2R_{x_1}\right). \tag{6}$$

The equation set is solved in the space

$$1 \le \xi \le \left(R_{x_2}\Big/R_{x_1}\right)^{1/2} \tag{7}$$

$$0 \le \eta \le \infty \tag{8}$$

$$0 \le \tau \tag{9}$$

The equations are first order in time and are integrated from a Blasius initial condition at $\tau = 0$

$$g = \xi f = \xi f_{\text{Blasius}} \tag{10}$$

The four boundary conditions in the $\eta$-dimension are

$$g = g_{\eta} = 0; \quad \eta = 0 \tag{11}$$

$$\left.\begin{aligned} g/\xi &= f = \eta - \beta \\ \Omega &= 0 \end{aligned}\right\} \eta \to \infty \tag{12}$$

where $\beta$ is a constant characteristic of the displacement thickness.

The upstream boundary conditions in $\xi$ are a linear combination of the Blasius solution and a time periodic solution of the Orr-Sommerfeld equation.

$$g = f_{Blasius} + A\ Re[\phi(\eta)\ exp(-i\omega\tau)]$$
$$g_\xi = f_{Blasius} - 2A\alpha Im[\phi(\eta)\ exp(-i\omega\tau)] \tag{13}$$

where $\phi$ is the Orr-Sommerfeld solution and A is some fixed amplitude. The real part of the dimensionless wave number, $\alpha$, and the real part of the dimensionless frequency, $\omega$, are defined in terms of the corresponding dimensional quantities

$$\omega = \bar{\omega} x_1 / U_\infty, \qquad \alpha = \bar{\alpha} x_1 \tag{14}$$

The third order system in $\xi$ requires only one downstream boundary condition

$$g_{\xi\xi\xi} = 0 \tag{15}$$

These equations are solved using a spectral method in both space dimensions; a form of Chebyshev polynomial expansion is used in each dimension. The solution is updated in time with an explicit finite difference scheme.

## 3. NUMERICAL RESULTS

In Ref. 8, the numerical results were restricted to one case with the emphasis on a comparison of the small and large amplitude Tollmien-Schlichting waves. In this report, the earlier work is extended to include: (1) calculations with additional physical parameters which show that the results in Ref. 8 may be somewhat atypical, (2) calculations with a longer streamwise region in order to better characterize the nonlinear behavior, and (3) details of the flow in the region where the behavior is very different from that assumed in nonlinear stability theory analyses.

As an introduction, consider three related figures taken from Murdock[8]. These figures depict calculations in which a periodic Orr-Sommerfeld disturbance is introduced into the boundary layer at an x-Reynolds number of $10^5$ with a dimensionless frequency given by

$$\omega = \bar{\omega} x_1 / U_\infty = 13.19 \tag{16}$$

Figure 1 shows the normalized amplitude of the perturbation velocity well down in the shear layer at some time after the Tollmien-Schlichting waves have propagated through the domain. The solid curve corresponding to a small amplitude disturbance has, as expected, a behavior very similar to a modulated sinusoid. The dotted curve shows substantial effects of nonlinear distortion and a small change in wave speed. A significant feature of Fig. 1 is that the positive peak of the large amplitude wave is bulged to the right upstream of $R_x = 1.7 \times 10^5$ and bulged to the left further downstream.

It is difficult to extract information from waveforms, such as those shown in Fig. 1; therefore, these solutions have been Fourier transformed in time. The time Fourier transformed version of Fig. 1 given in Fig. 2 shows that the amplitude variation of the nonlinear primary mode is not changed very much from its linear counterpart. This behavior is in agreement with the usual nonlinear stability theory. Up to a Reynolds number of about $1.3 \times 10^5$, the growth rate of the nonlinear wave (considering the energy in the first two modes) is greater than the growth rate of the linear wave. The possibility of this type of behavior is also contained in nonlinear stability theory. However, the behavior of the second mode beyond $R_x = 1.3 \times 10^5$ was unexpected in that the amplitude first decays and then grows again, the minimum occurring at about $R_x = 1.7 \times 10^5$. The minimum of the second mode in Fig. 2. occurs at about the same location as the change in nonlinear wave form in Fig. 1.

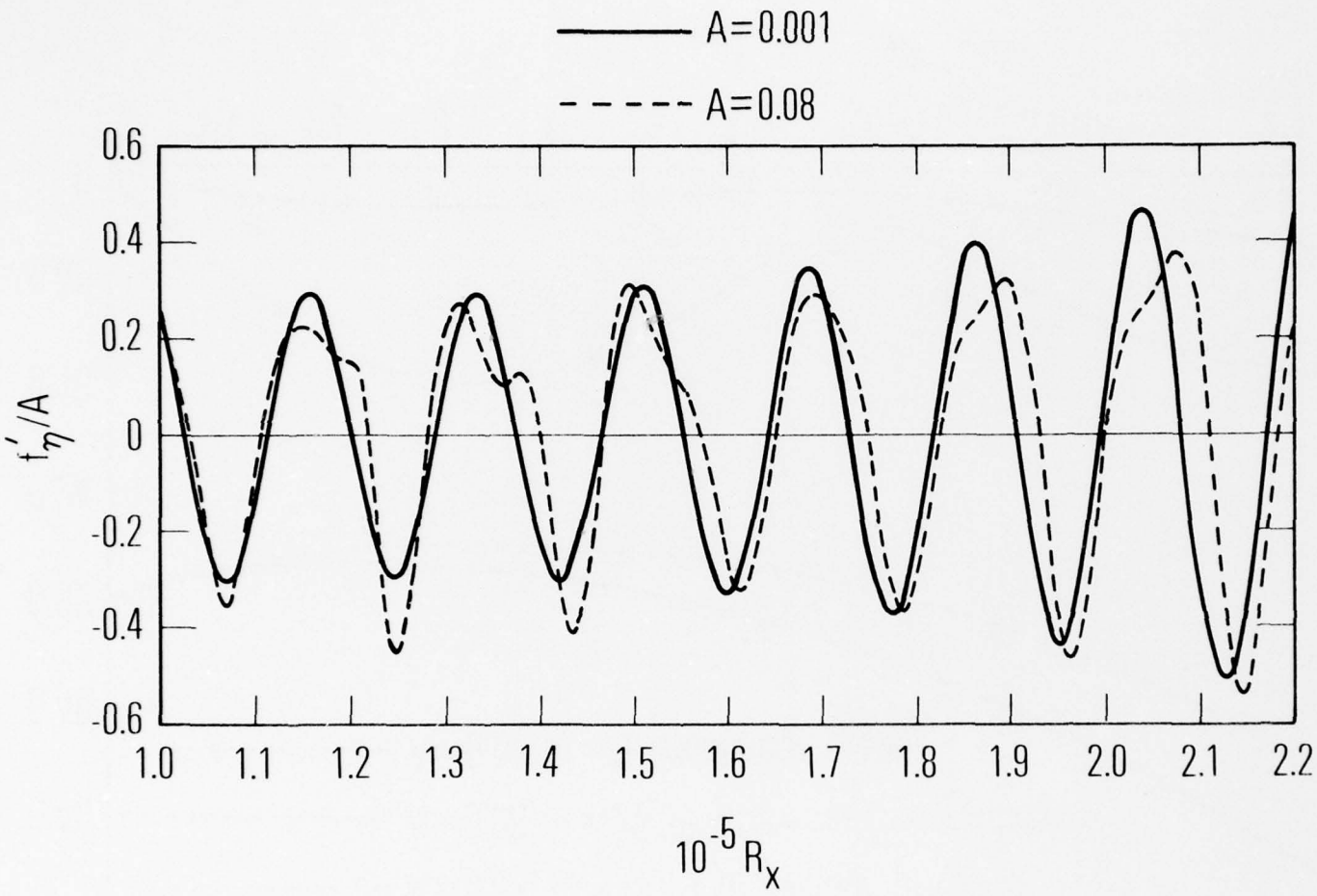


Fig. 1. Perturbation Velocity at $\eta = 0.2$, $\tau = 4.2265$

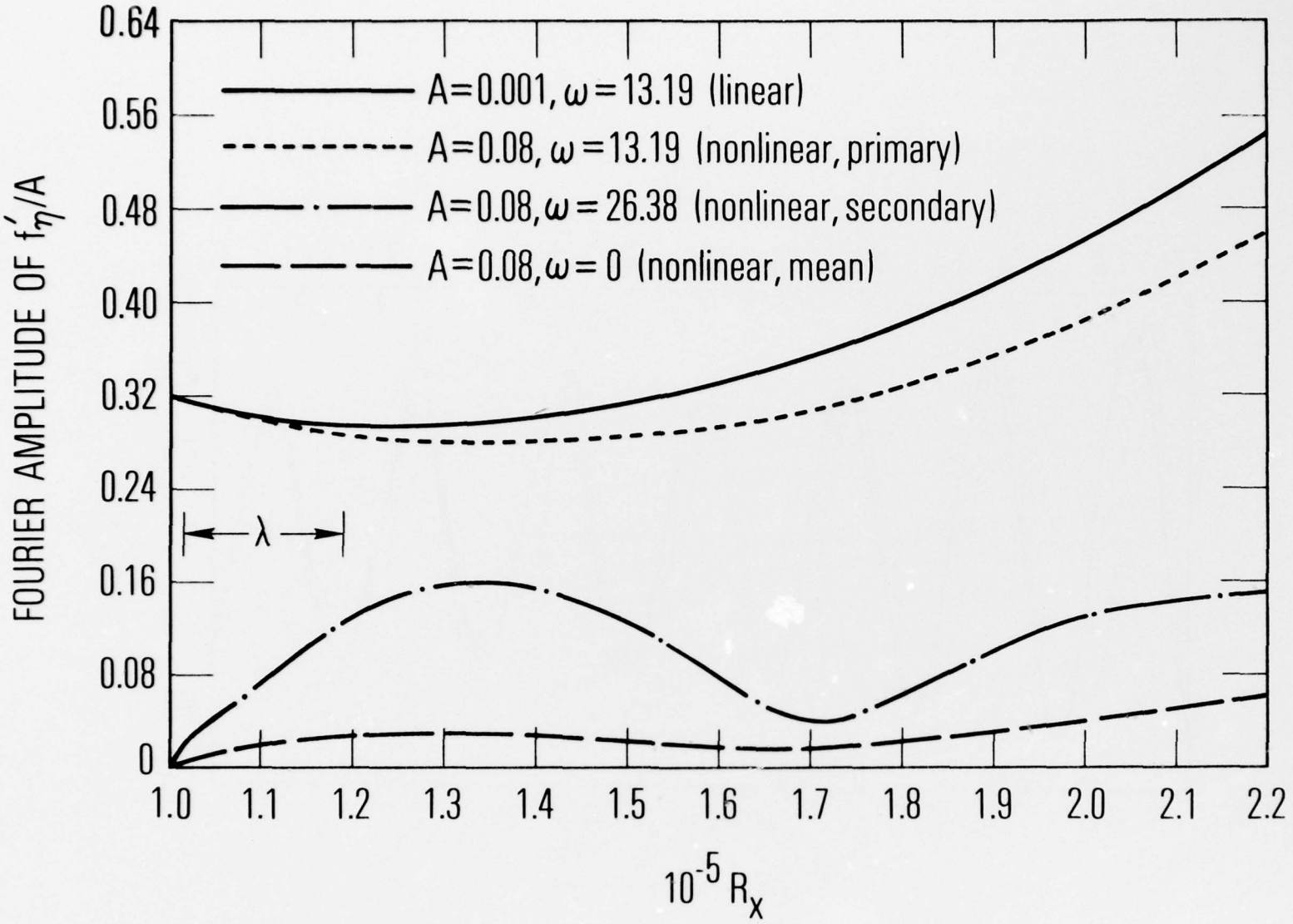


Fig. 2. Fourier Transformed Velocity at $\eta = 0.2$

Although the behavior in Figs. 1 and 2 is related, the change in wave shape in Fig. 1 cannot be explained on the basis of Fourier amplitude alone but must also depend on the relative phase of the first two modes. Accordingly, Fig. 3 shows the sine of the phase angle of the first two modes as a function of Reynolds number for the same conditions as Figs. 1 and 2. In nonlinear stability theory, it is always assumed that the second temporal harmonic is also a second spatial harmonic. If every other minimum of the dotted curve in Fig. 3 coincided with the minimums of the solid curve, then the dotted curve in Fig. 3 would be a spatial harmonic of the solid one. The figure shows that at $\eta = 0.2$ the nonlinear theory assumptions are in good agreement with the numerical solution. The dotted curve is slightly to the right of the location where a harmonic curve would be upstream of $R_x = 1.7 \times 10^5$ and then shifts abruptly to the left downstream of that station. This phase behavior is consistent with Fig. 1 in which the bulge shifted from right to left at $R_x = 1.7 \times 10^5$.

Figures 4, 5 and 6 show results similar to that presented in the first three figures for a higher Reynolds number and a higher dimensionless (lower dimensional) frequency with approximately the same amplitude of the Orr-Sommerfeld upstream boundary condition. Figure 4 demonstrates that there is significant distortion of the wave due to nonlinear effects, but in contrast to Fig. 1 the bulge is always to the left of the peak. The Fourier amplitudes are plotted in Fig. 5; the second mode again has a relative minimum but not nearly as dramatic as the one in Fig. 2. Finally, as expected from Fig. 4, Fig. 6 shows no significant variation in the relative phase. From these results, it is concluded that the first set of solutions may be atypical in that the second mode has a sharp minimum correlated with a phase shift; nevertheless, these solutions are more interesting precisely because of this unexpected behavior. Consequently, the remainder of the paper will be devoted to describing in detail the first solution, with emphasis on the region in the flow in which it differs qualitatively from both the second solution and nonlinear stability theory.

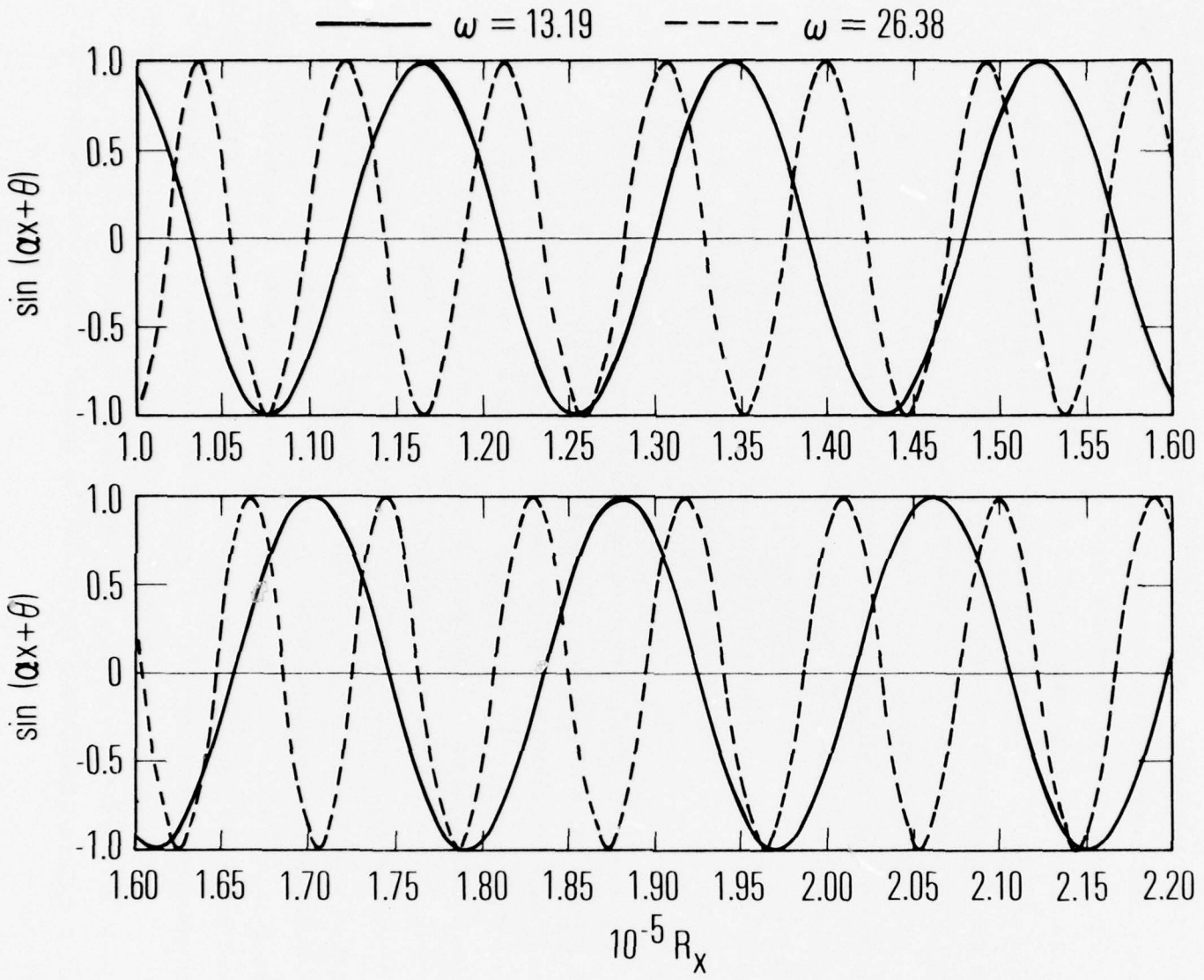


Fig. 3. Sine of the Phase Angle of the Primary and Secondary Wave at $\eta = 0.2$

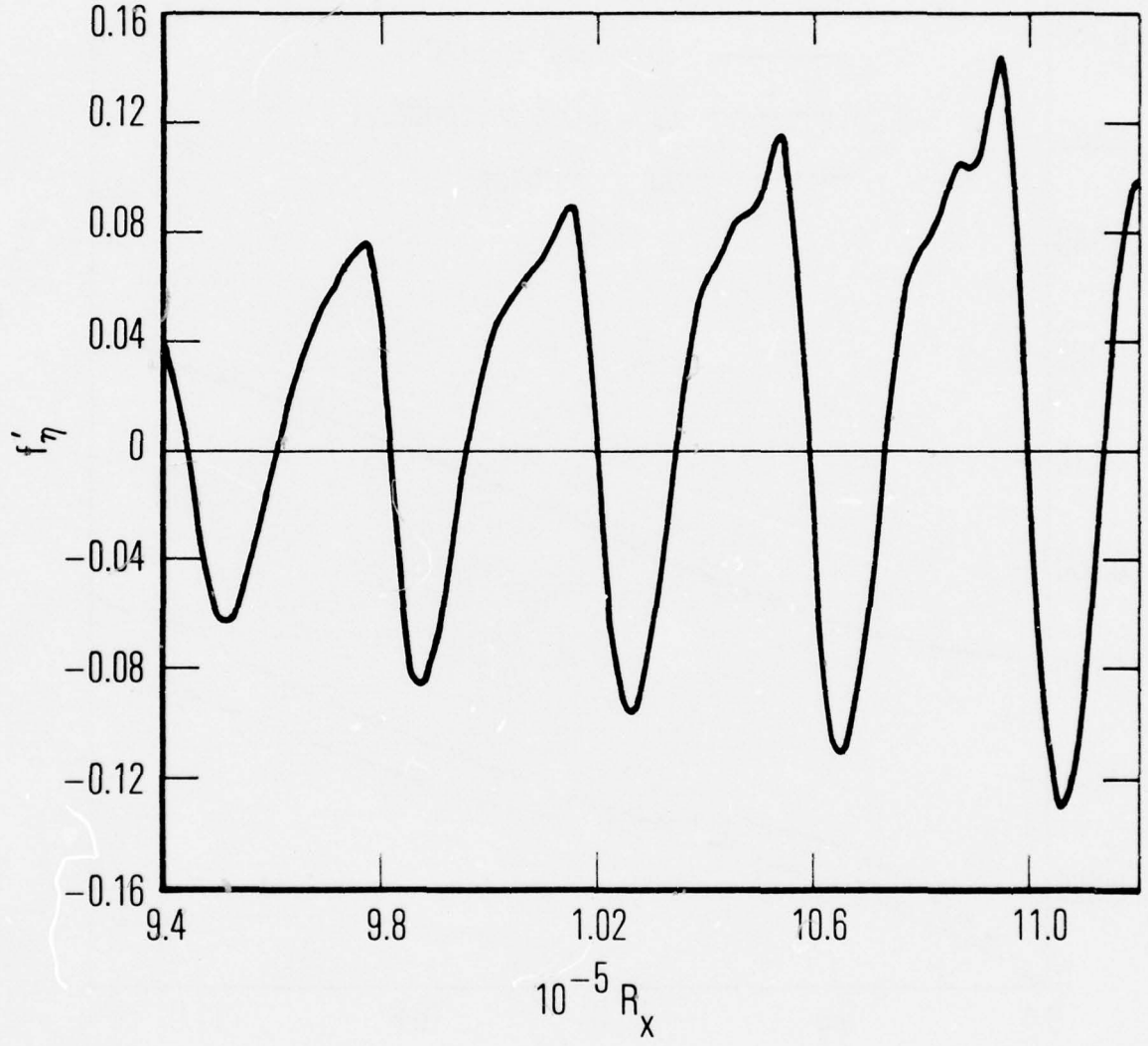


Fig. 4. Perturbation Velocity at $\eta = 0.2$

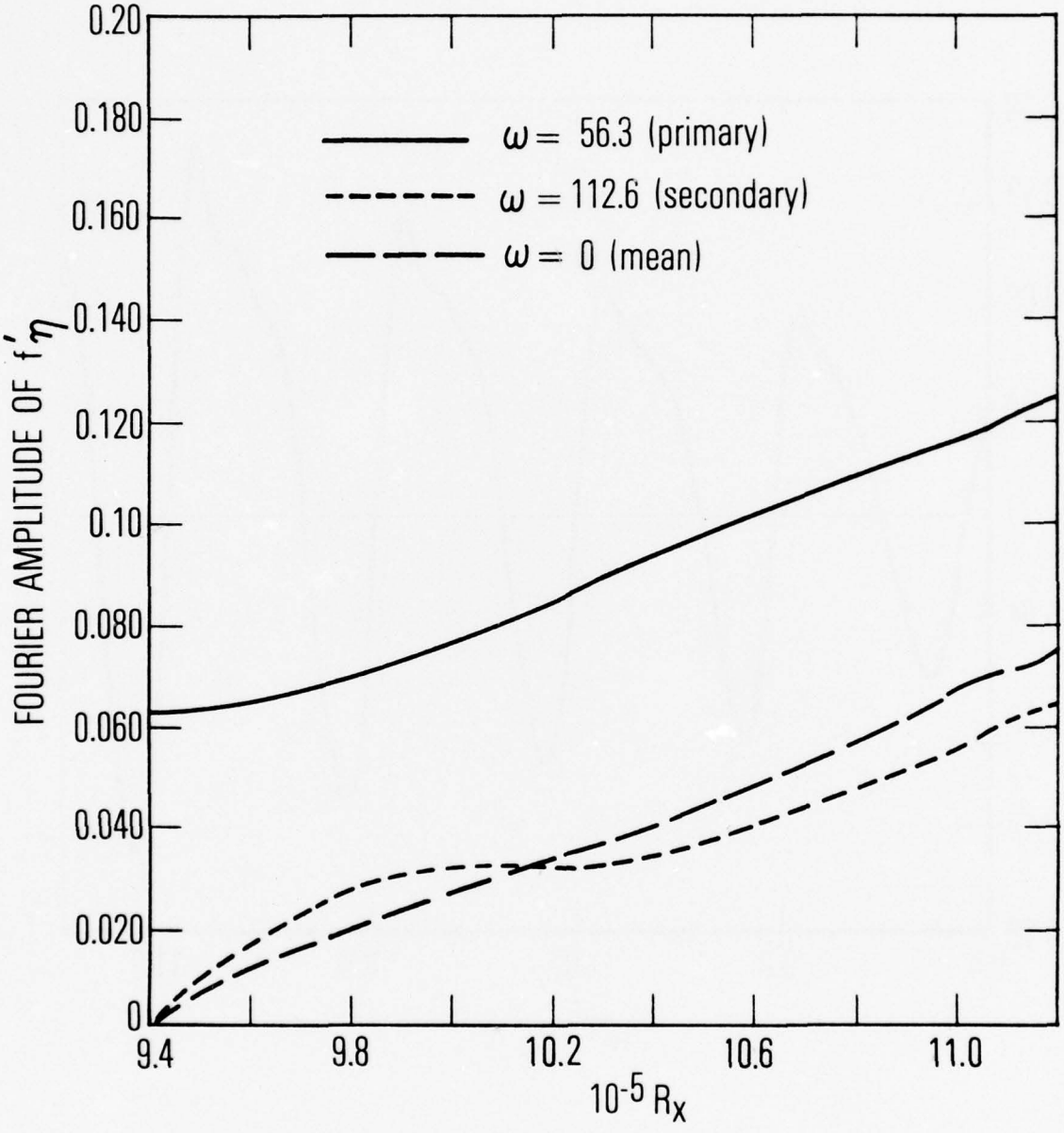


Fig. 5. Fourier Transformed Velocity at $\eta = 0.2$

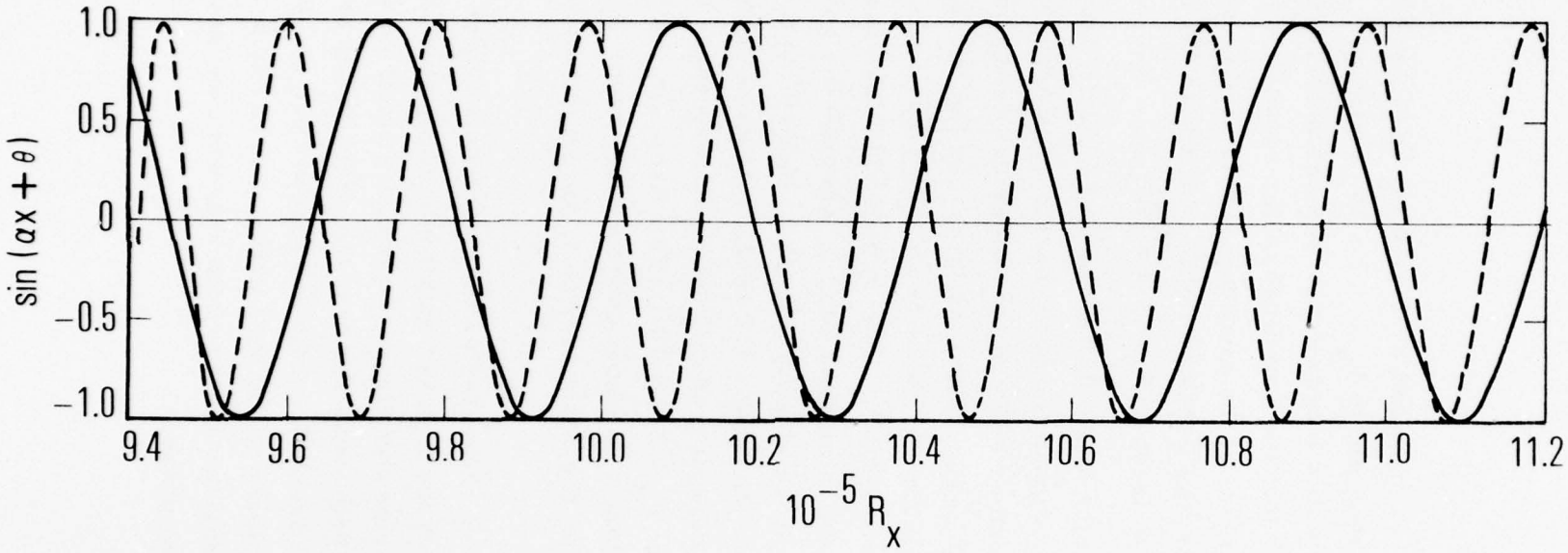


Fig. 6. Sine of the Phase Angle of the Primary and Secondary Wave at $\eta = 0.2$

One obvious question raised by Fig. 2 is, Does the amplitude of the second mode grow subsequent to $R_x = 2.2 \times 10^5$ or is there another minimum? A calculation with a longer range in x has been completed, and the results in Fig. 7 show that the amplitude of the second mode increases monotonically downstream of the minimum. It is also found that there are no further phase shifts; the behavior for $R_x > 1.7 \times 10^5$ in Figs. 1 and 3 persists downstream at least to $R_x = 2.8 \times 10^5$.

The phase behavior at $\eta = 0.2$ shown in Fig. 3 is, as was noted, very much as expected; the second temporal harmonic is very nearly a second spatial harmonic. Further study of the numerical solutions has shown that the results illustrated in Fig. 3 are not typical of the whole boundary layer. The solutions demonstrate that there is an anomalous region for $1.0 \lesssim \eta \lesssim 1.8$ in the vicinity of $R_x \approx 1.7 \times 10^5$. The anomaly is illustrated in Figs. 8 and 9. Figure 8 is qualitatively similar to Fig. 3, although the phase variation of the secondary at $\eta = 0.8$ in the vicinity of $R_x \approx 1.74 \times 10^4$ is more rapid than elsewhere. The phase plot at $\eta = 1.0$ (Fig. 9) is quite different; one complete oscillation cycle has disappeared and the secondary curve tracks the primary curve in a region near $R_x = 1.7 \times 10^5$. This behavior, with one less oscillation cycle than expected, is present out to a value of $\eta = 1.8$. At $\eta = 2.0$ and beyond, the behavior of the secondary is again consistent with nonlinear stability theory.

In order to better characterize the anomalous region, it is useful to look at the variation of the Fourier amplitude of the velocity across the boundary layer. The behavior away from the region of interest is as shown in Figs. 10 and 11. In both these figures, the shape of the secondary is very similar to that of the primary except for the fact that the maximum and phase reversal points are closer to the wall in the case of the secondary. As the figures show, this behavior appears both upstream and downstream of the region with anomalous phase.

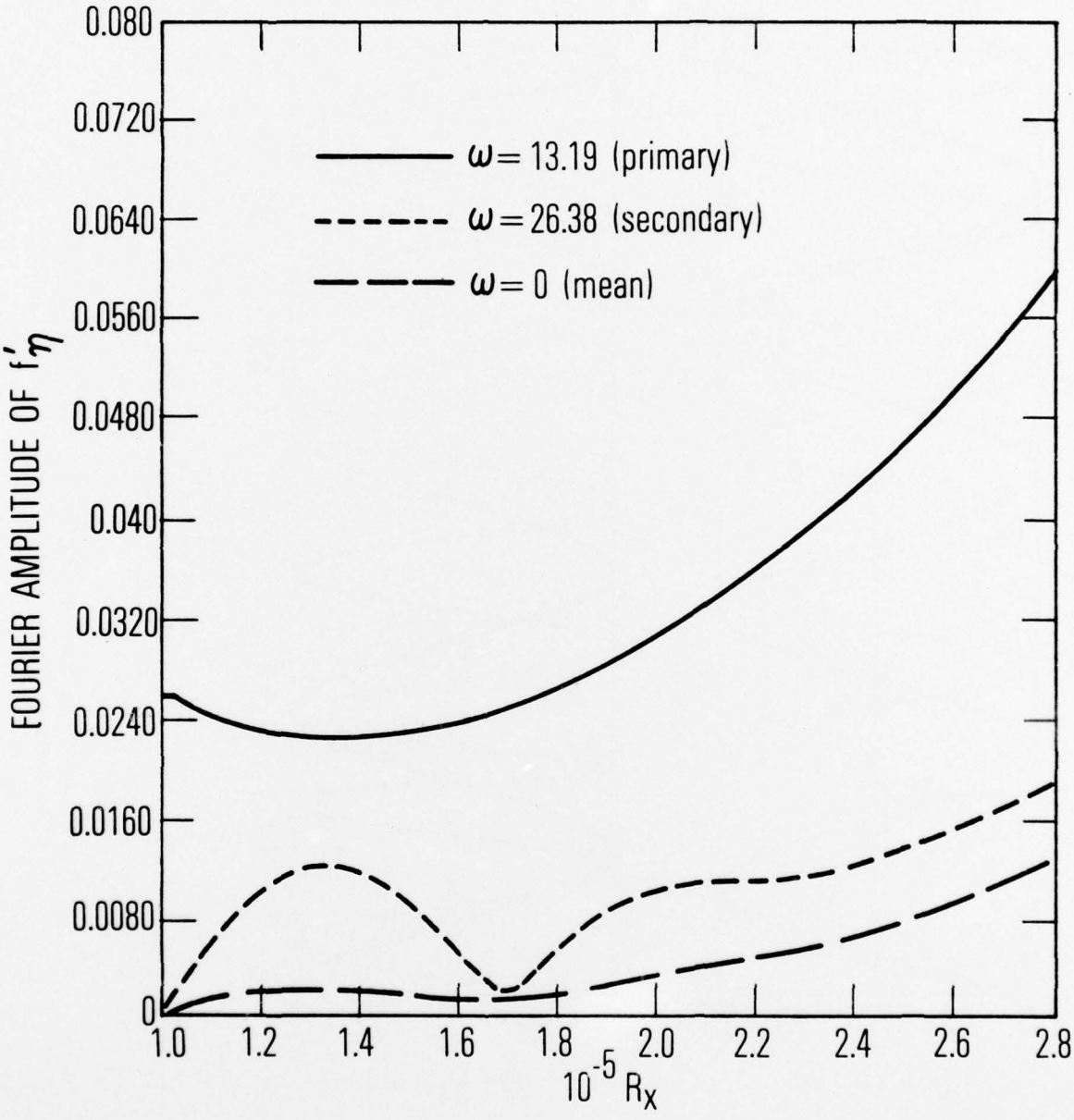


Fig. 7. Fourier Transformed Velocity at $\eta = 0.2$

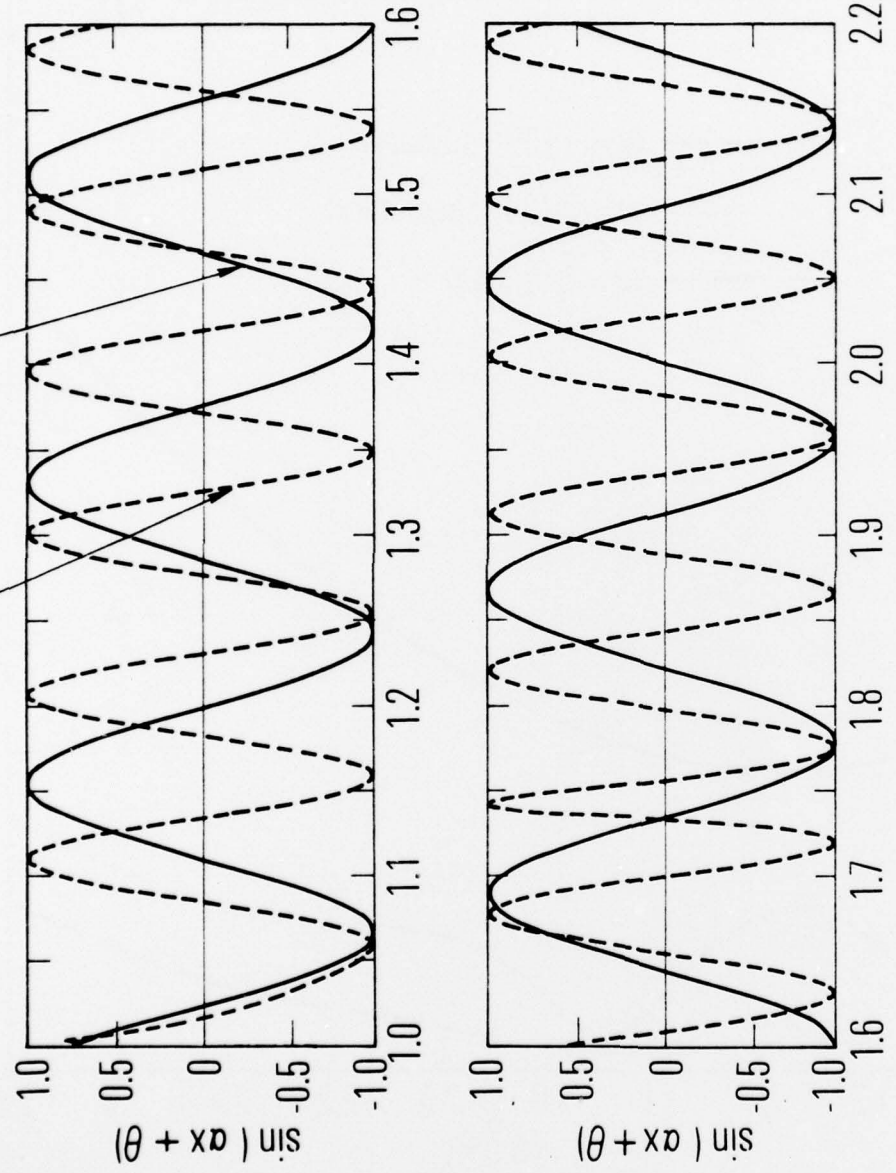


Fig. 8. Sine of the Phase Angle of the Primary and Secondary Wave at $\eta = 0.8$

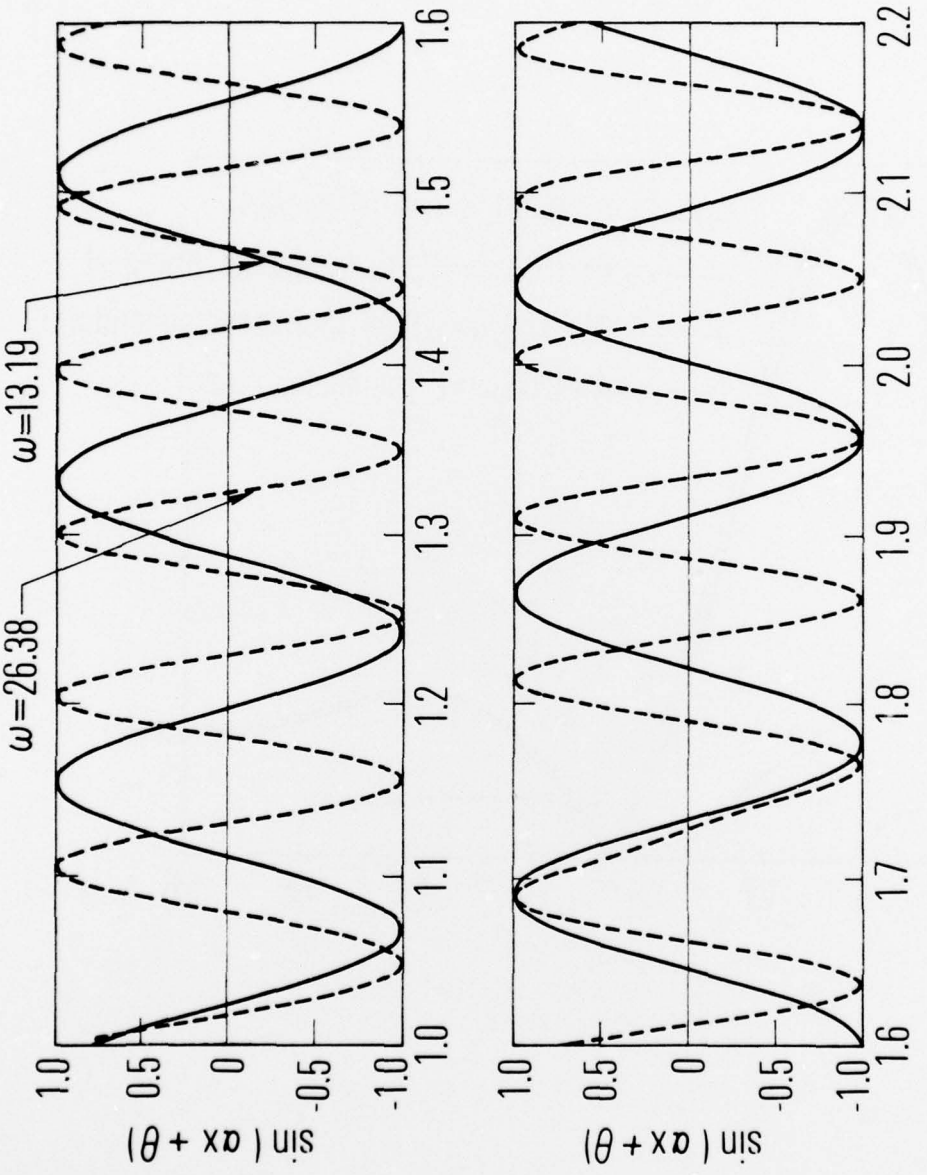


Fig. 9. Sine of the Phase Angle of the Primary and Secondary Wave at $\eta = 1.0$

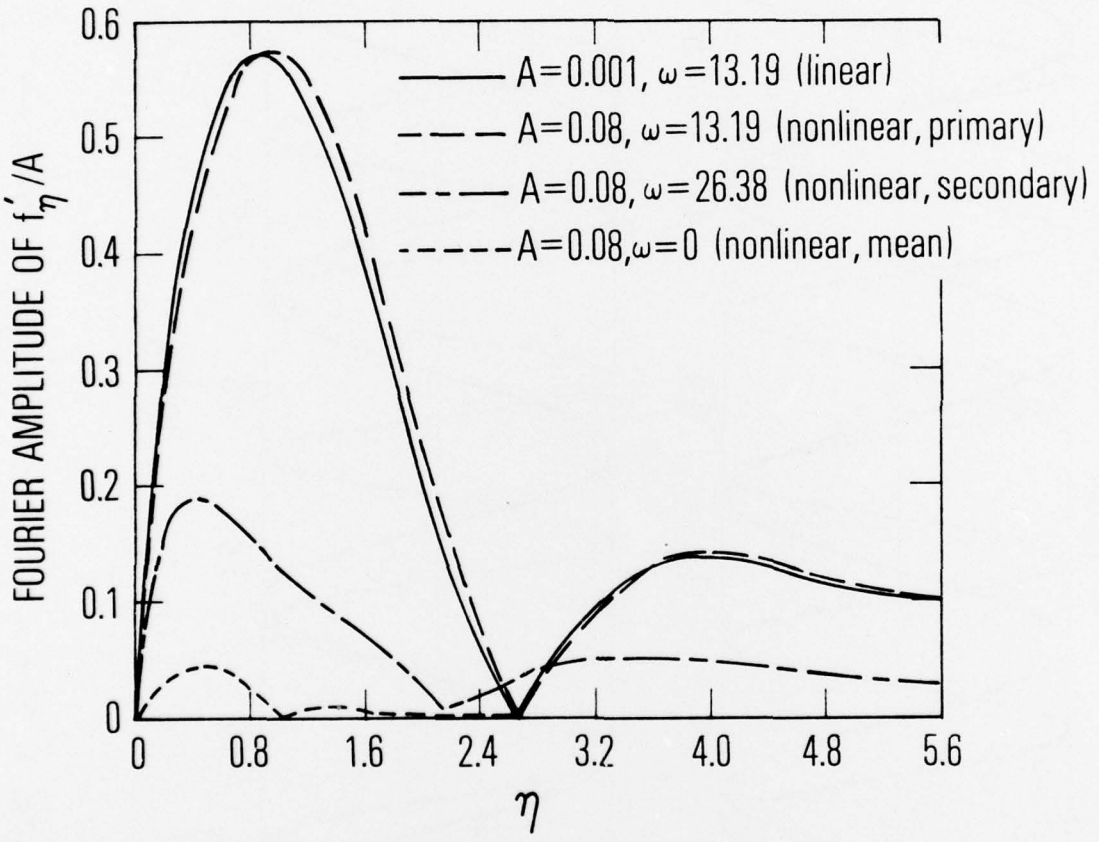


Fig. 10. Normalized Fourier Amplitudes at $R_x = 1.3 \times 10^5$

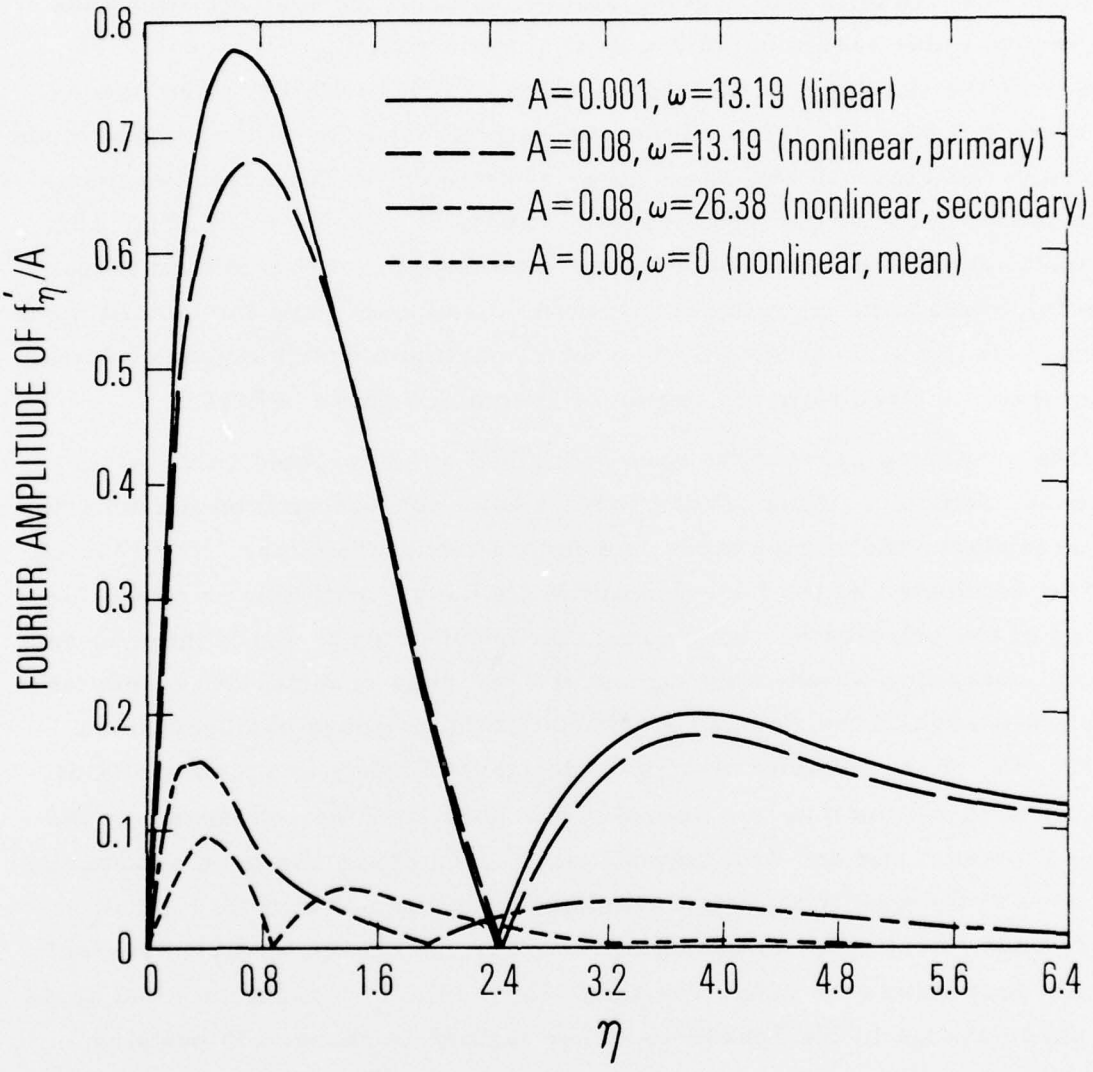


Fig. 11. Normalized Fourier Amplitudes at $R_x = 2.2 \times 10^5$

The Fourier amplitudes of both the first and second modes in the vicinity of $R_x = 1.7 \times 10^5$ have been plotted; there is no significant variation of the first mode in this region, but the shape of the Fourier amplitude of the second mode varies rapidly with $R_x$ in this region. Figures 12, 13 and 14 show the variation of the second mode profiles with $R_x$. The second mode at $R_x = 1.62 \times 10^5$ (Fig. 12) has the typical behavior of the second mode as shown in the Figs. 10 and 11. Going downstream, a third relative maximum develops between $\eta$ of about one and two; at $R_x = 1.74 \times 10^5$ (Fig. 13), the atypical structure is best developed. Downstream of this station (Figs. 13 and 14), the additional relative maximum disappears, and the second mode returns to its more usual shape. The third maximum which appears between $\eta$ of about one and two is in the region of anomalous phase behavior.

The preceding paragraphs have described an unexpected behavior of the second harmonic. Although the results have concentrated on the behavior of the secondary, the second mode is a forced mode; therefore, its behavior should be dominated by the behavior of the primary. With this in mind, the behavior of the primary has been carefully investigated to see if there is any change in character which could explain the previous results. As noted, no significant change in the Fourier amplitude of the primary has been found. However, the phase behavior is another matter. Figure 15 shows a plot of the phase of $f'_\eta$ versus $\eta$ at two Reynolds numbers, one well upstream of the region of interest and one well downstream. (The phase has been arbitrarily set to zero at the wall to facilitate comparison of the two curves.) At $R_x = 10^5$, the phase first rises to nearly $\pi/4$; then in the "phase reversal region" the phase decreases to a value less than $-3\pi/4$. At $R_x = 2.2 \times 10^5$, the slope of the phase change in the "phase reversal region" is changed to positive, and the phase increases from a nominal $\pi/4$ to $5\pi/4$ (shown as $-3\pi/4$ in the figure). Although plots of Fourier amplitude suggest that there is a "phase reversal point," curves such as those in Fig. 15 show that in fact the phase change occurs over a finite region and may have either a positive or a negative slope. These results are consistent with solutions of the Orr-Sommerfeld

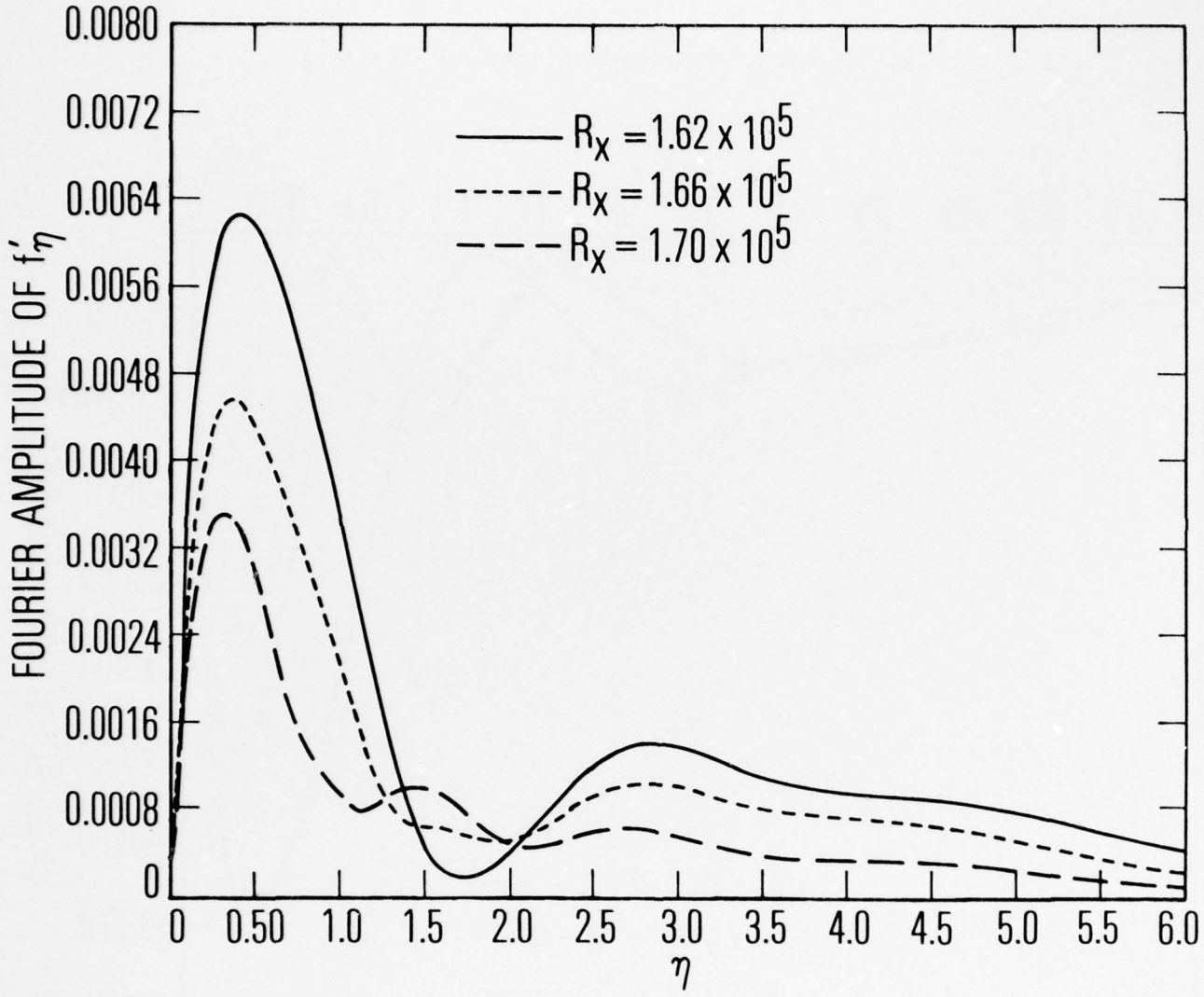


Fig. 12. Fourier Amplitude of Second Mode

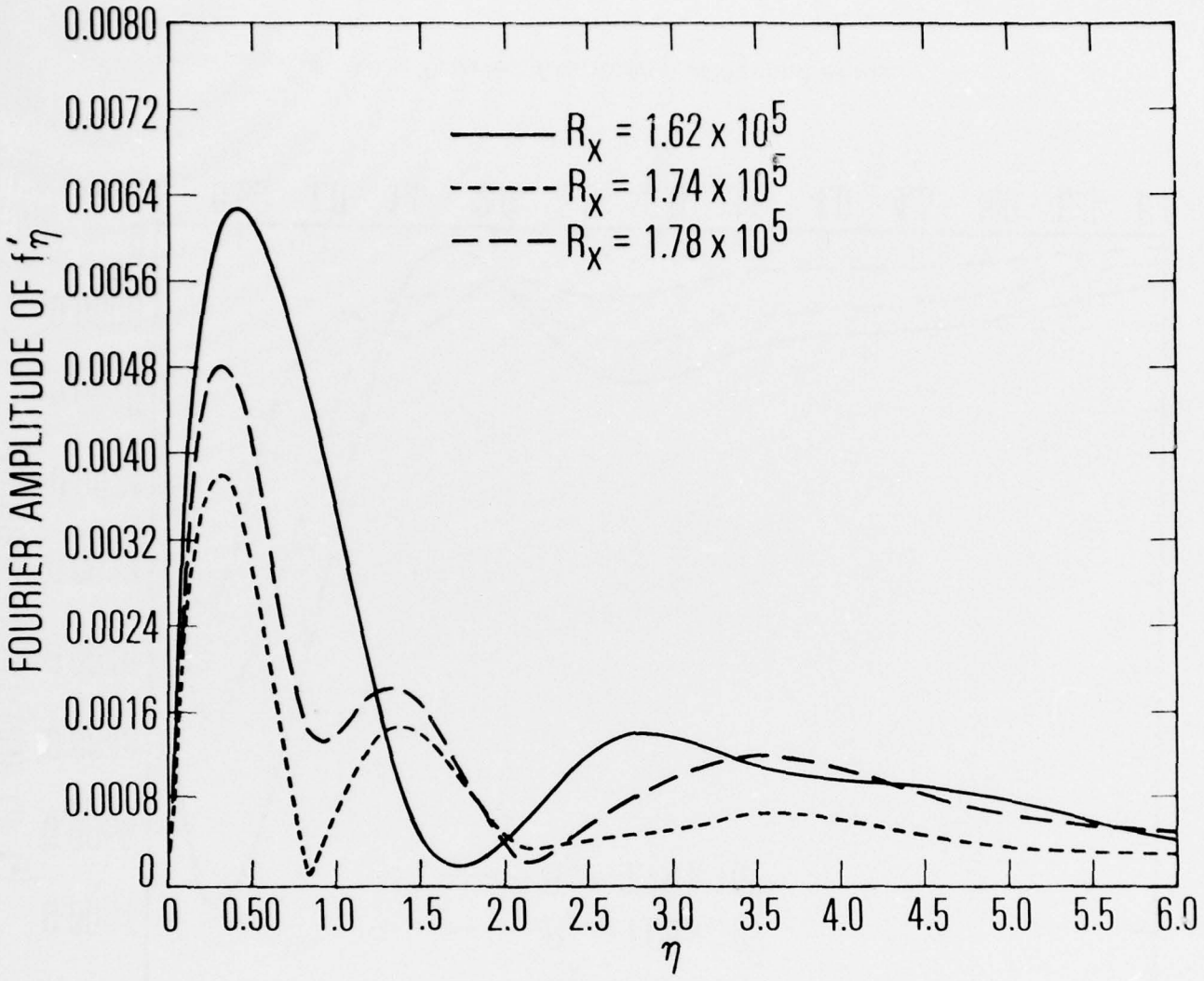


Fig. 13. Fourier Amplitude of Second Mode

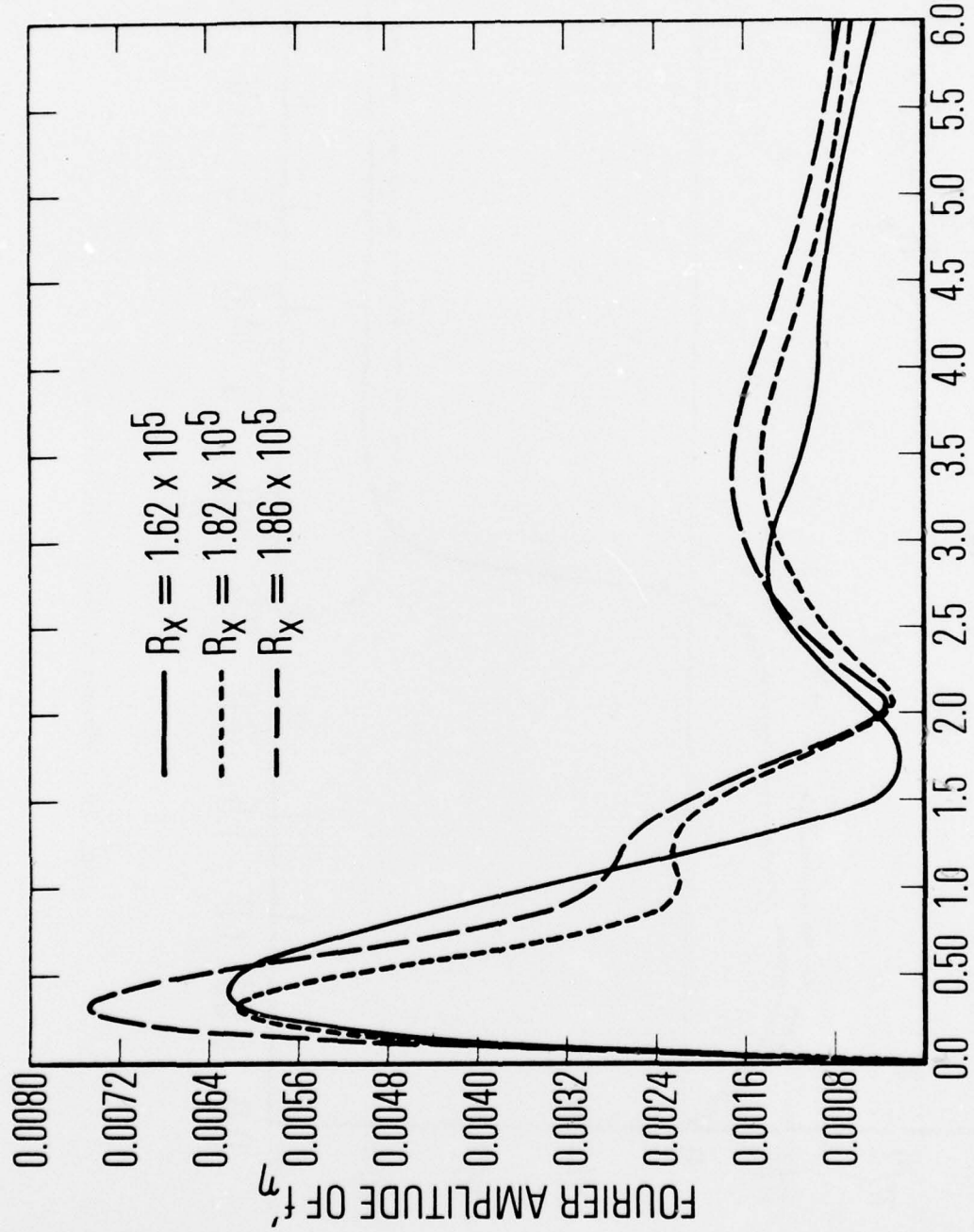


Fig. 14. Fourier Amplitude of Second Mode

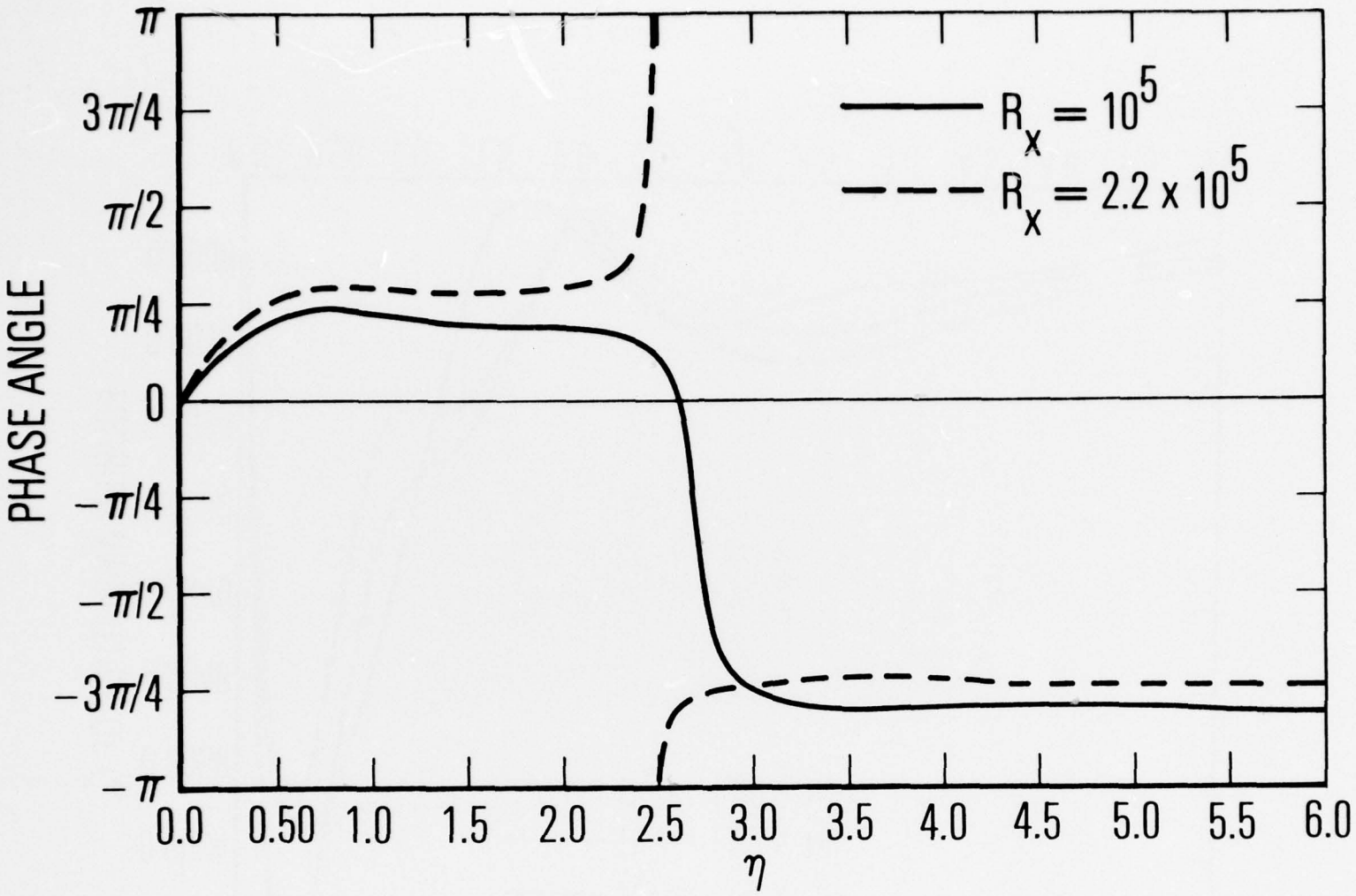


Fig. 15. Phase Angle of the Primary

equation. In order for the phase reversal to occur at a point, both the real and imaginary parts of that solution would have to be zero at the same point. This is in general not true--a rapid phase change does occur in the vicinity of the zero of the real part because the imaginary part is much smaller than the real part. Solutions to the Orr-Sommerfeld equation demonstrate that the outermost zero of the imaginary part (of $d\phi/dy$) moves out with increasing Reynolds number relative to the zero of the real part. When the zero of the imaginary part is closer to the wall than that of the real part, the phase change has a negative slope (similar to Fig. 15 at $R_x = 10^5$). When the zero of the imaginary part is outside that of the real part, the phase change has a positive slope.

Figure 15 shows that the phase behavior of the primary mode changes character in the solution region. A careful inspection of curves such as those in Fig. 15 shows that in the present solution the change in behavior occurs at $R_x = 1.71 \times 10^5$. This correlates very well with the location of the minimum amplitude point of the second harmonic in Fig. 2. Because it is believed that the primary must control the secondary and because the change in the phase behavior of the primary occurs in the anomalous region, it is concluded that this phase behavior causes the anomalous behavior of the secondary.

It should be noted that the flow region which is not in qualitative agreement with nonlinear stability theory is localized in both space dimensions. The Reynolds number based on a Tollmien-Schlichting wave length for the present problem is about $2 \times 10^4$, and so the anomaly is confined to roughly one wave length. As noted, the region of interest is also confined to values of $\eta$ between one and two. This fact implies that one-dimensional wave theories, such as nonlinear stability theory, cannot predict the details of such regions in which the wave phenomena are clearly not one-dimensional. The existence of such a region could be predicted by linear stability theory because the first mode is reasonably well modeled by the linear theory.

A possible criticism of the present results is that the upstream boundary condition is somewhat artificial. This is true because a large amplitude pure sinusoidal disturbance is imposed upstream. In any real flow situation in which a large amplitude disturbance developed either from being amplified or from external noise sources, the higher modes would be present. On the other hand, the present calculation is a well defined and repeatable method of learning about the nonlinear flow behavior. It is also reasonable to assume that far anough downstream of the upstream boundary, the details at that boundary are unimportant. It seems likely that the present results are not far enough from the upstream boundary to be independent of it, although further numerical studies are required to quantify this conjecture. A final point is that the results presented here illustrate a new and unexpected solution which may lead to a better understanding of high Reynolds number flows, regardless of how these flows are created.

Another question which should be addressed is, Are the present results real or are they somehow caused by the numerics? There is no evidence that numerical errors have influenced the present results. Reference 8 shows comparisons of various calculations which lend credence to the results. Subsequent to the publication of that paper, the longer streamwise calculation shown in Fig. 7 was completed. A comparison of Figs. 3 and 7 illustrates the agreement of these two calculations over their common range of validity. However, the numerics do impose a limit on the amount of information which can be extracted from the solution. In particular, the phase curves (e.g., Figs. 8 and 9) are obtained by dividing one component of the Fourier amplitude by its absolute value. When these numbers are small, the resultant phase curves may be in error. Phase plots which attempt to show the details intermediate between Figs. 8 and 9 would possibly be in error. However, the amplitude of the second mode is certainly large enough to be meaningful at values of $\eta$ like 0.4 and 1.5 (see Figs. 12, 13 and 14). At these values of $\eta$, the phase behavior is similar to that of Figs. 8 and 9. Thus, it is concluded that the numerics are accurate enough to predict the presence of the anomalous region, but the details of the phase going from one region to another are uncertain.

## 4. CONCLUDING REMARKS

The numerical results presented herein provide insight into the behavior of nonlinear Tollmien-Schlichting waves. Although the solutions are qualitatively similar to those of nonlinear stability theory in most regions, flows incompatible with one-dimensional wave models are also found to exist. The details of the first and second temporal harmonics are presented with an emphasis on the anomalous region. It is argued that the first harmonic drives the secondary and, therefore, must control it everywhere. A change in the phase behavior of the primary occurs in the anomalous region, and it is suggested that this change causes the anomaly. Because the first mode is reasonably well modeled by linear stability theory, this theory may be used to predict the approximate location of the type of anomalous region described herein.